


Comprehensive analysis of resilience of human airway epithelial barrier against short-term PM_{2.5} inorganic dust exposure using in vitro microfluidic chip and ex vivo human airway models

Ozlem Goksel^{1,2}  | Meryem Irem Sipahi³ | Sena Yanasik⁴  | Pelin Saglam-Metiner^{2,4} | Sema Benzer⁴ | Leila Sabour-Takanlou⁵ | Maryam Sabour-Takanlou⁵ | Cigir Biray-Avci⁵ | Ozlem Yesil-Celiktas^{2,4,6}

¹Department of Pulmonary Medicine, Division of Immunology and Allergy, Laboratory of Occupational & Environmental Respiratory Diseases and Asthma, Faculty of Medicine, Ege University, Izmir, Turkey

²Translational Pulmonary Research Center (EgeSAM), Ege University, Izmir, Turkey

³Department of Biotechnology and Biomedicine, Technical University of Denmark, Kongens Lyngby, Denmark

⁴Department of Bioengineering, Faculty of Engineering, Ege University, Izmir, Turkey

⁵Department of Medical Biology, Faculty of Medicine, Ege University, Izmir, Turkey

⁶METU MEMS Center, Ankara, Turkey

Correspondence

Ozlem Goksel, Department of Pulmonary Medicine, Division of Immunology and Allergy, Laboratory of Occupational & Environmental Respiratory Diseases and Asthma, Faculty of Medicine, Ege University, Izmir 35100, Turkey.
Email: ozlem.goksel@ege.edu.tr

Abstract

Background and Objective: The updated World Health Organization (WHO) air quality guideline recommends an annual mean concentration of fine particulate matter (PM_{2.5}) not exceeding 5 or 15 µg/m³ in the short-term (24h) for no more than 3–4 days annually. However, more than 90% of the global population is currently exposed to daily concentrations surpassing these limits, especially during extreme weather conditions and due to transboundary dust transport influenced by climate change. Herein, the effect of respirable <PM_{2.5} inorganic silica particle exposures on epithelial barrier integrity was simultaneously evaluated within the biomimetic microfluidic platform-based airway epithelial barrier (AEB)-on-a-chip and human bronchoscopic ex vivo airway tissue models, comparatively.

Methods: Silica particles at an average size of 1 µm, referred to as <PM_{2.5}, dose-dependently tested by MTT and LDH analyses. The elicited dose of 800 µg/mL was applied to human airway epithelial cells (Calu-3) seeded to the membrane at air-liquid interface in the AEB-on-a-chip platform, which is operated under static and dynamic conditions and to ex vivo human bronchoscopy bronchial tissue slices for 72 h. For both models, healthy and exposed groups were comparatively investigated. Computational fluid dynamics simulations were performed to assess shear stress profiles under different flow conditions. Qualitative and quantitative analyses were carried out to evaluate the resilience of the epithelial barrier via cell survivability, morphology, barrier integrity, permeability, and inflammation.

Abbreviations: AEB, airway epithelial barrier; A549, human alveolar basal epithelial adenocarcinoma cells; ACE2, angiotensin-converting enzyme 2; ARG1, arginase 1; BEAS-2B, human bronchial epithelium cells; BSA, bovine serum albumin; Calu-3, human airway epithelial cells; CD31/PECAM-1, platelet endothelial cell adhesion molecule-1; CFD, computational fluid dynamics; COPD, Chronic obstructive pulmonary disease; DAPI, 4',6-diamidino-2-phenylindole; dc, dynamic control; dsp, dynamic silica particles; ELISA, enzyme-linked immunosorbent assay; FBS, fetal bovine serum; FITC, Fluorescein Isothiocyanate; IF, immunofluorescence; IFN, interferon; IL, interleukin; iNOS, inducible NO synthase; LDH, lactate dehydrogenase; MTT, 2,5-diphenyl-2H-tetrazolium bromide; OD, optical density; PBS, phosphate-buffered saline; PCLS, precision-cut lung slices; PCNA, proliferating cell nuclear antigen; PDMS, polydimethylsiloxane; PET, polyethylene terephthalate; PFA, paraformaldehyde; PM, particulate matter; PMMA, polymethyl methacrylate; qRT-PCR, real-time quantitative reverse transcription PCR; sc, static control; RT, room temperature; SEM, scanning electron microscopy; sp, silica particles; ssp, static silica particles; STAT-6, signal transducer and activator of transcription 6; THP-1, a human monocytic cell line; TNF, tumor necrosis factor; WST, Water-Soluble Tetrazolium; ZO-1, zonula occludens; U937, human pre-monocytic cell line.

This is an open access article under the terms of the [Creative Commons Attribution-NonCommercial](https://creativecommons.org/licenses/by-nc/4.0/) License, which permits use, distribution and reproduction in any medium, provided the original work is properly cited and is not used for commercial purposes.

© 2024 The Author(s). Allergy published by European Academy of Allergy and Clinical Immunology and John Wiley & Sons Ltd.

Ozlem Yesil-Celiktas, Department of Bioengineering, Faculty of Engineering, Ege University, Izmir 35100, Turkey.
Email: ozlem.yesil.celiktas@ege.edu.tr

Funding information

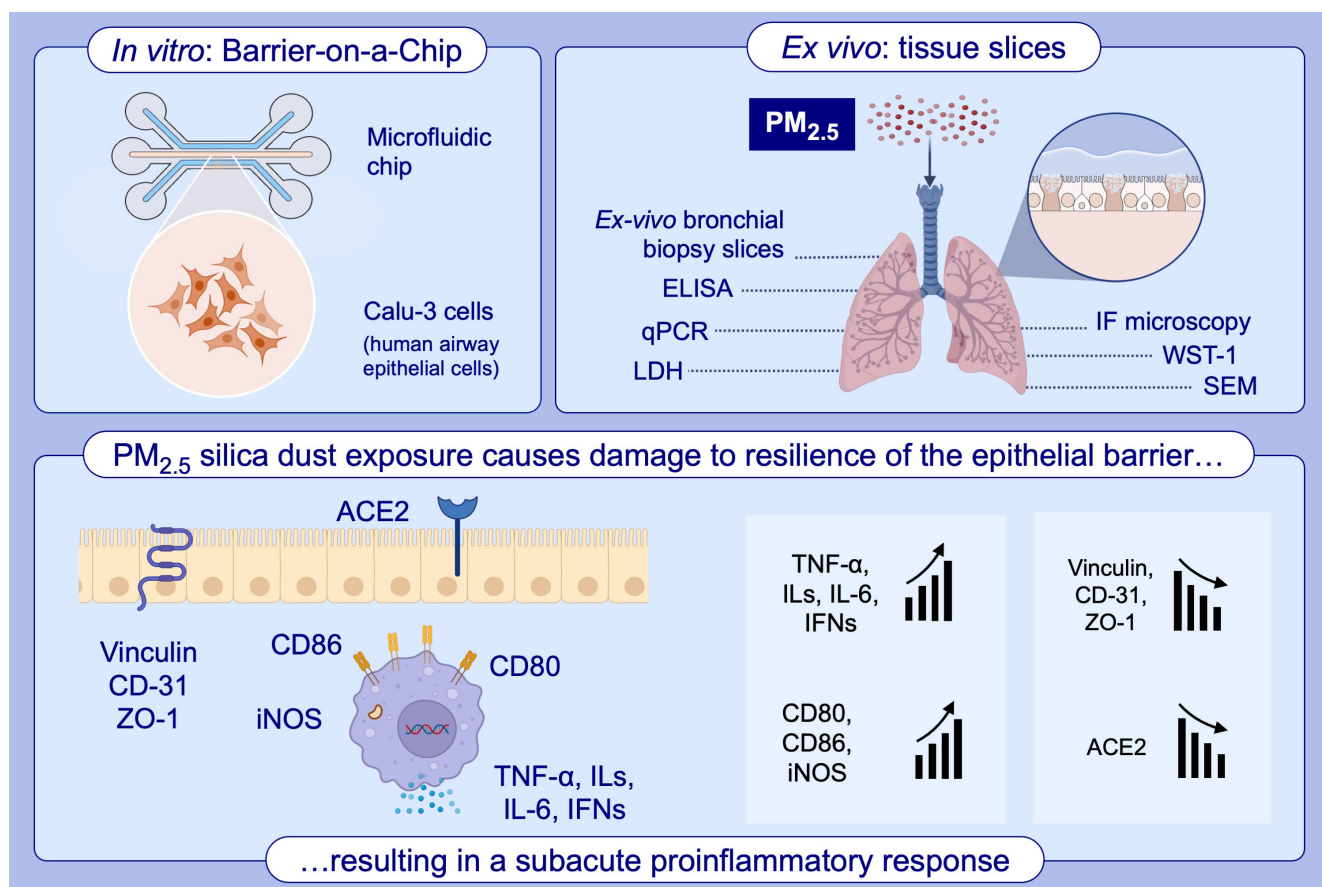
Presidency of the Republic of Turkey Strategy and Budget Department, Grant/Award Number: 2019K12-149080; Scientific and Technological Research Council of Turkey (TUBITAK), Grant/Award Number: 1139B412102522

Results: In the AEB-on-a-chip platform, short-term exposure to 800 µg/mL PM_{2.5} disrupted AEB integrity via increasing barrier permeability, decreasing cell adhesion-barrier markers such as ZO-1, Vinculin, ACE2, and CD31, impaired cell viability and increased the expression levels of proinflammatory markers; *IFNs*, *IL-6*, *IL-1s*, *TNF-α*, *CD68*, *CD80*, and *Inos*, mostly under dynamic conditions. Besides, decreased tissue viability, impaired tissue integrity via decreasing of *Vinculin*, *ACE2*, *β-catenin*, and *E-cadherin*, and also proinflammatory response with elevated *CD68*, *IL-1α*, *IL-6*, *IFN-γ*, *Inos*, and *CD80* markers, were observed after PM_{2.5} exposure in ex vivo tissue.

Conclusion: The duration and concentration of PM_{2.5} that can be exposed during extreme weather conditions and natural events aligns with our exposure model (0–800 µg/mL 72 h). At this level of exposure, the resilience of the epithelial barrier is demonstrated by both AEB-on-a-chip platform emulating dynamic forces in the body and ex vivo bronchial biopsy slices. Lung-on-a-chip models will serve as reliable exposure models in this context.

KEYWORDS

airway epithelial barrier, microfluidic systems, particulate matter, PM_{2.5}, silica particles



GRAPHICAL ABSTRACT

Biomimetic microfluidic platform-based dynamic AEB-on-a-chip model developed in order to recapitulate PM_{2.5} silica particle exposure. Quantitative and qualitative characterization tests were carried out for cell barrier disruption and inflammatory immune responses. Our easy-to-use AEB-on-a-chip model and ex vivo bronchial biopsy slices were investigated comparatively. Abbreviations: ACE2, angiotensin-converting enzyme 2; AEB, airway epithelial barrier; Calu-3, human airway epithelial cells; ELISA, enzyme-linked immunosorbent assay; IF, immunofluorescence; IFN, interferon; IL, interleukin; iNOS, inducible nitric oxide synthase; LDH, lactate dehydrogenase; PM_{2.5}, particulate matter <2.5 µm; qPCR, quantitative polymerase chain reaction; SEM, scanning electron microscopy; TNF-α, tumor necrosis factor α; WST, water-soluble tetrazolium; ZO-1, zonula occludens

1 | INTRODUCTION

The concept of planetary one health as “One Earth, One Family, One Future” directs attention to the extreme degradation of our planet due to anthropogenic activities. Ever-increased global warming, climate change and natural destructive events pose significant health concerns as extreme weather events and dust storms are becoming more frequent and severe. Studies suggest that annual dust aerosol concentrations have increased worldwide due to increased desert dust and sandstorms.^{1–5} Respiratory exposure to these dust particles, especially particulate matter (PM); <PM_{2.5} and PM₁₀, has been implicated not only in chronic respiratory diseases, asthma, and chronic obstructive pulmonary disease (COPD) but also in allergic rhinitis, conjunctivitis, ischemic heart, cardiovascular, and neurodegenerative diseases.⁶ Among the 204 studies included in a recently published epidemiologic review, most of them (84.8%) reported having significant associations between desert dust and adverse health effects, mainly for respiratory and cardiovascular mortality and morbidity causes.⁷

The WHO recently updated their air quality guideline for annual PM_{2.5} exposure from 10 to 5 µg/m³, citing global health considerations.⁸ But limits are largely unattainable for many parts of the world, even with extreme abatement efforts, given that the natural background alone often exceeds 5 µg/m³. Both climate change, by modulating natural PM_{2.5} sources, and transboundary transport of dust might further interrupt efforts to achieve these limits in different geographical regions. It has been reported that even under an extreme abatement scenario, with no anthropogenic emissions, more than half of the world's population would still experience annual PM_{2.5} exposures above the 5 µg/m³ guideline (including >70% and >60% of the African and Asian populations, respectively), largely due to fires and natural dust.⁹ In the immediate wake of a strong dust event, atmospheric PM₁₀ concentrations can reach or exceed 1000 µg/m³ while PM_{2.5} concentration can be above 500 µg/m³.¹⁰ In the Sohar region, these storms were the biggest in over a decade and caused extremely high levels of PM_{2.5} that exceeded 350 µg/m³ and reached up to 1884 µg/m³ from time to time.¹¹ Global Atmospheric Watch Regional Observatory at Lamezia, Italy and The Copernicus Atmosphere Monitoring Service forecasts reported PM_{2.5} levels that exceed 100 µg/m³ for some dusty days with high atmospheric pressure.¹² Basically, owing to the exceptionally high ambient concentrations of PM that are experienced during extreme weather conditions, atmospheric level of PM can range from 100 to 6000 µg/m³. Those atmospheric events typically endure for 2–3 days, aligning with the WHO's definition of short-term exposure as measured over minutes to days. Short-term exposure to such silica PM can also occur during natural disasters such as earthquakes, floods, and collapses. Additionally, workers and residents face the risk of long-term exposure, measured as a mean of one or several years, to high levels of dust due to anthropogenic activities like substandard construction and demolition practices in rapidly expanding urban areas, as well as in coal mines and other occupational settings.

The AEB is crucial with respect to the body's defense against harmful substances, as it acts as a physical and chemical barrier between the body and the external environment. It is mainly composed of a single

layer of cells, tightly packed and connected by tight junctions, which help to prevent the passage of harmful substances. Besides, airway epithelial cells directly sense pathogens and respond defensively, which is a frontline component of the innate immune system with specificity for different pathogen classes.¹³ Thus, AEB has been one of the target sites in the respiratory tract, and research efforts have been devoted to the development of in vitro models to investigate the effects of various toxicants such as smoke^{14–16} exhaust,¹⁷ nanoparticles,¹⁸ PM,¹⁹ and viral infections.^{20–22} The current models span from Transwells to more complex and physiologically relevant microfluidic platforms, enabling culturing of human small airway epithelial cells and endothelial cells.^{23,24} These models provide in-depth information on the pathophysiology of airway remodeling, as well as the genetic and epigenetic characteristics which reflect the interaction between intrinsic and environmental signals.^{25,26} In urban regions with extreme weather conditions, natural destructive events or anthropogenic pollution, the uncontrollably high PM_{2.5} dust limits may exceed the values recommended by WHO's regulations for health. In this guideline for health risk assessments, exposures are defined on different time domains as, long-term exposure, measured as a mean of one or several years; and short-term exposure, measured over minutes to days. The aim of this study was to evaluate short-term acute–subacute exposure of high concentrations of <PM_{2.5} inorganic dust to the resilience of the epithelial barrier in both in vitro microfluidic based human AEB-on-a-chip platform and ex vivo human bronchial biopsy material slices, comparatively in a physiologically relevant manner. Prior to the experiments, flow conditions were simulated to determine the shear stress effects of respirable PM_{2.5} on epithelial cells. Subsequent to dose-dependent <PM_{2.5} administration to lung epithelial cells, the cytotoxic concentration of PM_{2.5} dust was determined and the resilience of the epithelial barrier along with inflammatory responses including cytokines *IL-6* and *IL-10* as well as changes in gene expression levels indicating the alterations in the barrier integrity, permeability, morphology, survivability, and immune response.

2 | MATERIALS AND METHODS

Briefly, commercial raw silica microparticles were sterilized, and particle size distributions were measured using Zetasizer. The elicitation of cell lines among Calu-3, A549, and BEAS-2B for in vitro on-chip model and effective dose of PM_{2.5} for the in vitro and ex vivo models were assessed by MTT and LDH assays. Besides Calu-3 cells, THP-1 and U937 monocytes were used to evaluate immune cell response against PM_{2.5} and to check endotoxin level of the particles by applying the lowest concentration. The microfabrication of the airway epithelial barrier-on-a-chip platform was carried out by replica molding of PDMS. The CFD simulations were performed in COMSOL Multiphysics to examine the diffusion of PM_{2.5} and the resulting shear stress profiles under flow conditions. Calu-3 cells-based static and dynamic AEB-on-chip models were formed, and a PM_{2.5} exposed model was evaluated to determine the epithelial cell damage, barrier disruption, and inflammatory response with WST-1, LDH, ELISA, qRT-PCR, IF, FITC permeability, and SEM imaging. Finally, lung transbronchial biopsy samples were taken,

and the dynamic ex vivo biopsy slice cultures were performed in parallel to the on-chip model to evaluate PM_{2.5} exposure and were subsequently characterized using LDH, ELISA, IF, and qRT-PCR analyses.

All detailed materials and methods are available online as Appendix S1 in the Supporting Information section.

3 | RESULTS

3.1 | PM_{2.5} administration alters the epithelial cell viability and increases immune response in a dose and cell-type-dependent manner

The average particle sizes of silica particles were 960 nm (Figure 1A); thus, they have been attributed as PM_{2.5}, which refers to particulate matter with a diameter of fewer than 2.5 micrometers.

Exposures of Calu-3, A549, and BEAS-2B cells to PM_{2.5} at doses ranging between 50 and 800 µg/mL were investigated, where significant differences in cell viability and cytotoxicity were observed. The lowest dose of 50 µg/mL PM_{2.5} exposure led to a reduction of ~30% ($p < .0001$) (Figure 1B), ~10% ($p > .05$), and ~70% ($p < .0001$) (Figure S1A) in cell viability of Calu-3, A549, and BEAS-2B cells, respectively. On the other hand, the highest dose of 800 µg/mL PM_{2.5} exposure resulted in ~50% ($p < .0001$), ~30% ($p < .001$), and ~75% ($p < .0001$) inhibition in Calu-3, A549, and BEAS-2B cells compared to the untreated controls. As for LDH release associated with cytotoxicity, the lowest dose of 50 µg/mL PM_{2.5} exerted lower than ~1% ($p > .05$) (Figure 1C), ~5% ($p > .05$), and ~10% cytotoxicity (Figure S1B), whereas the highest dose of 800 µg/mL PM_{2.5} elevated to ~6.5% ($p < .0001$), ~20% ($p < .0001$) and ~25%, for Calu-3, A549, and BEAS-2B cells, respectively. When the light microscopy images were examined, it was observed that the cells exposed to

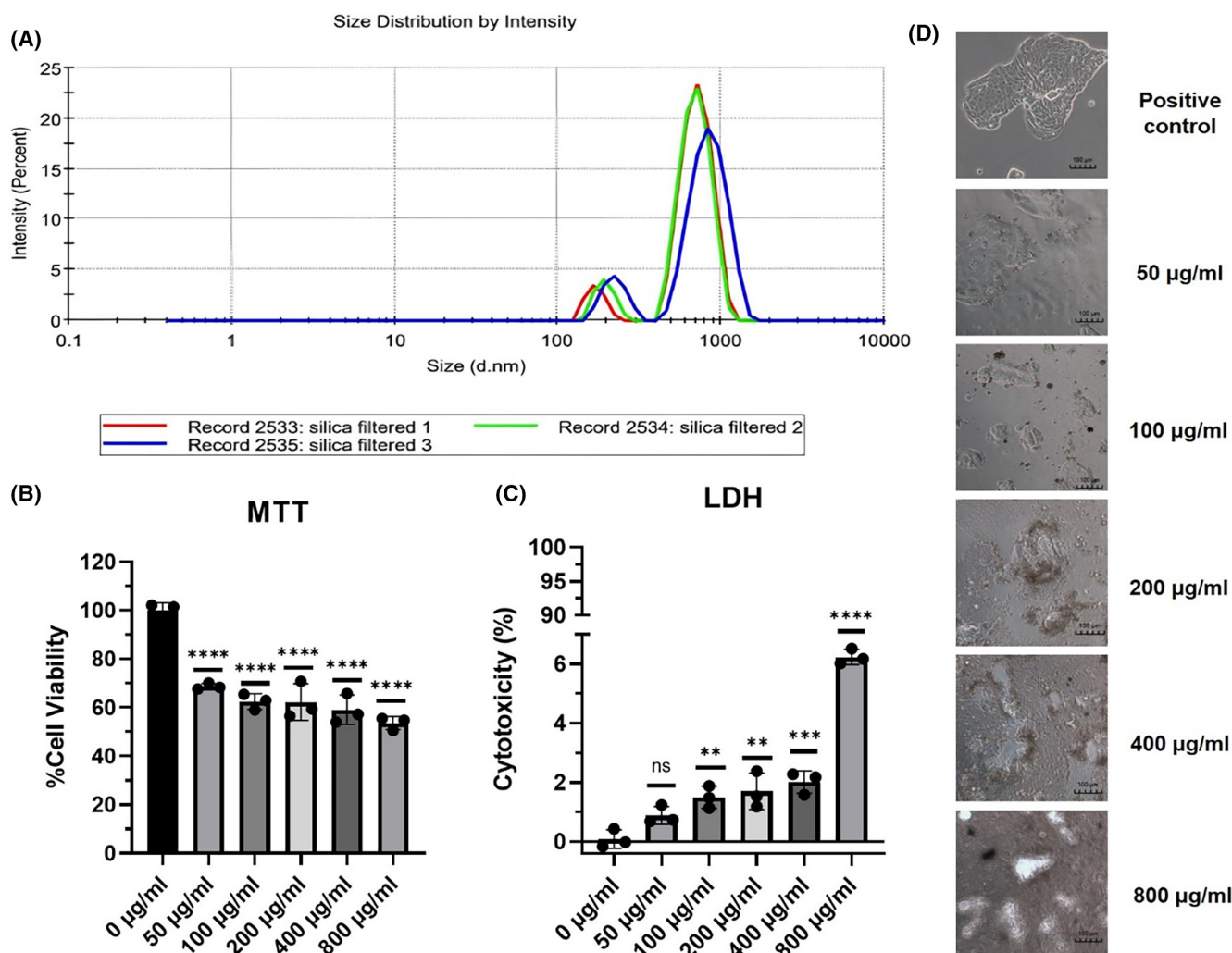


FIGURE 1 Exposure to PM_{2.5} negatively affects cell viability by exerting a cytotoxic effect on Calu-3 cells. (A) Particle size distribution of PM_{2.5}. (B) MTT assay results of Calu-3 cells exposed to different doses of PM_{2.5} (**** $p < .0001$ different doses groups vs control group (0 µg/mL), $n = 3$ for independent replicates = 2) (C) LDH activity results of Calu-3 cells exposed to different doses of PM_{2.5} (ns $> .05$, ** $p < .01$, *** $p < .001$, **** $p < .0001$ different doses groups vs control group (0 µg/mL), $n = 3$ for independent replicates = 2). (D) The bright-field microscopic images of Calu-3 cells exposed to different doses of PM_{2.5} (Motic AE31E, bar scale: 100 µm, $n = 2$ for independent replicates = 2).

PM2.5 had disrupted and irregular morphologies in comparison to untreated control cells (Figure 1D, Figure S1C).

Considering these results, among the epithelial cell lines commonly used in human in vitro AEB studies,^{25,27-29} BEAS-2B cells were too sensitive, and A549 cells were quite resistant to PM2.5 exposure in this study, where Calu-3 cells were shown quite morphological, physiological, and biological compatibility upon to PM2.5 exposure as a most proper cell type for using in vitro AEB-on-a-chip model. The effective dose for the in vitro on-chip model and ex vivo model was also determined as 800 µg/mL.

In addition to Calu-3 cells, THP-1, and U937 monocytes were used to evaluate immune cell responses against PM2.5 and to evaluate endotoxin levels by applying the lowest concentration of PM2.5. Compared to the control group, there were no clear changes in cell proliferation and morphology at the lowest concentration of 50 µg/mL. Besides, while immune cell activation and proliferation were observed in THP-1 monocytes, a decrease in cell viability due to cytotoxicity was observed in Calu-3 and U937 cells when exposed to high concentration of 800 µg/mL PM2.5 (Figure S2A). Endotoxins, such as lipopolysaccharides (LPS) derived from gram-negative bacteria, lead to the production of proinflammatory cytokines such as *IL-1β*, *TNFα*, and *IL-6*.³⁰⁻³² When *TNF-α* and *IL-1β* levels in cell supernatants were examined, an increase in cytokine levels were observed mostly in monocytes at high concentration of PM2.5, as expected. Besides, low concentration of PM2.5 were shown not to exert significant changes ($p < .05$) in endotoxin-sensitive proinflammatory cytokine levels compared to controls. Thus, this phenomenon suggested that commercial silica particles may not contain endotoxin and show proinflammatory activity due to PM2.5 cytotoxicity at increasing concentrations (Figure S2B).

3.2 | Diffusion of PM2.5 in human airway epithelial barrier-on-a-chip simulated through computational fluid dynamics

The diffusion of PM2.5 into the medium and the maximum shear stress created in the microfluidic platform were simulated by COMSOL Multiphysics software. In order to mimic the mixing of inhaled PM2.5 in the respiratory tract through the epithelium and into the blood, a model including the particle tracking of fluid flow and laminar flow interface and movement of particles with the liquid flow was created on the designed microfluidic platform. The microfluidic platform was designed to include a porous PET membrane sandwiched between two PDMS-based channels with softened corners to prevent particle accumulation and dead zones to mimic the human AEB (Figure 2A).

The flow rate in the dynamic conditions created in the microfluidic platform, the particle size and density were simulated in accordance with the initial conditions (Table S1). It was observed that the particles moved at a maximum speed of 4.97×10^{-3} m/s in the oscillation that occurs in the rocker system at a speed of 1 rpm for 30s (Figure 2B). Thus, it has been determined that the dynamic

conditions created can prevent the unwanted accumulation of particles and provide their maximum diffusion into the cells. In the simulation made to predict the maximum velocity that the particles given by homogenization in the nutrient medium can reach under dynamic conditions, the maximum flow velocity was determined to be 6.09×10^{-3} m/s, while the position of the particles in the microfluidic platform was examined. While moving from the initial position to the extreme position in the microfluidic platform, the velocity of the particles increased with the liquid flow, whereas the particles with similar velocities in the middle areas are positioned more homogeneously (Figure 2C). Simulation studies have been carried out to predict the shear stress that PM2.5 and flow conditions would exert on the cells forming an epithelial barrier in the microfluidic platform. While the maximum shear stress distribution is observed as 2×10^{-5} Pa in the end wall parts of the microfluidic platform, it is seen that the shear stress is distributed homogeneously in the middle areas where cell seeding occurs (Figure 2D). In addition, the particles were observed to act in accordance with the homogeneously distributed shear stress in the middle regions.

3.3 | Effect of PM2.5 in human airway epithelial barrier-on-a-chip differs under static and dynamic conditions

We developed a PET membrane-supported bidirectional rocker-shaked microfluidic platform that mimicked the cellular architecture and physiological environment of the lungs with air-liquid interface to examine the effects of PM2.5 arriving in the lungs through inhaled air on the human AEB. First of all, CellTracker green dye-labeled Calu-3 cells were seeded to the PET membrane in the PDMS-based microfluidic system, reached confluency for 3 days, stained with DAPI, and evaluated for forming an epithelial barrier in the microfluidic platform (Figure S3). To examine the effect of PM2.5 on AEB integrity, Calu-3 cells on-chip platform were exposed to PM2.5 at the same concentration and duration under static and dynamic conditions mimicking air-liquid interface. After 72h of exposure, the cell viability was significantly ($p < .0001$) reduced by ~65% in the PM2.5 administered group under dynamic conditions (dsp) and by ~45% under static conditions (ssp), compared to dynamic control (dc) and static control (sc) groups (Figure 3A) with some noticeable differences within themselves due to the influence of the dynamic flow conditions.

The cytotoxic LDH levels secreted from the plasma membrane after the cell apoptosis were also significantly increased ($p < .001$) as a result of the exposure to PM2.5, while a higher percentage of cytotoxicity was observed under dynamic conditions (Figure 3B). We further analyzed the pro- and anti-inflammatory cytokines by ELISA assay to evaluate the immune responses of Calu-3 cells to PM2.5. Indicative of the proinflammatory response, *IL-6* release was significantly increased ($p < .001$) to ~150 ng/L (~2-fold) under static conditions compared to control, while it was increased more significantly under dynamic conditions, both compared to its control (~twofold, $p < .0001$) and static condition ($p < .05$) (Figure 3C).

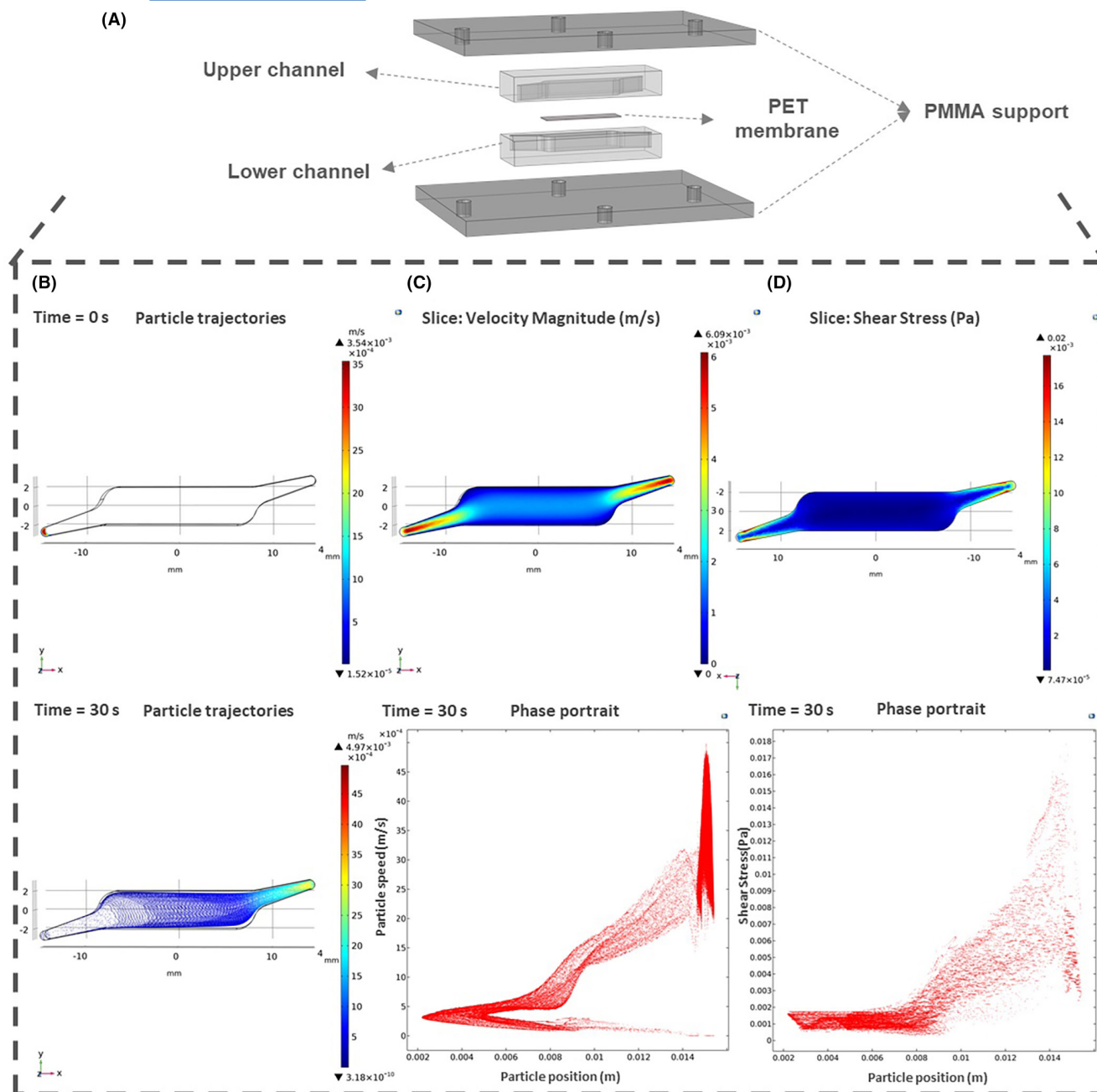


FIGURE 2 Dynamic flow conditions in the microfluidic platform ensure optimal diffusion of PM2.5. (A) Microfluidic platform design by COMSOL Multiphysics. (B) Velocities of dust particles in the microfluidic platform at 0 and 30 s. (C) Numerical simulation of velocity for the microfluidic platform and particle/velocity phase portrait. (D) Numerical simulation of shear stress for the microfluidic platform and particle/shear stress phase portrait.

Additionally, the release of *IL-10*, an anti-inflammatory cytokine, was reduced with PM2.5 exposure under both static ($p < .001$) and dynamic ($p < .0001$) conditions compared to their control groups, while this decrease was seen more in dynamic culture (Figure 3D). So that, in dynamic conditions, inflammatory response was better observed than in static conditions with higher increasing levels of *IL-6* and decreasing levels of *IL-10* compared to control groups. The effects of PM2.5 exposure on Calu-3 cells in both static and dynamic AEB-on-a-chip models, qRT-PCR analysis, was performed to determine mRNA expression levels of specific cell adhesion, survival and inflammatory markers (Figure 3E, Figure S4A,

Appendix S2a). It was observed that the expression levels of cell adhesion-related genes, mostly for *Vinculin* (6.87-fold) and *CD31* (4.06-fold) genes, were generally higher than under dynamic control groups, which aim to better mimic the epithelial barrier integrity as in vivo environment via fluidic flow, compared to the static control group. As expected, *ZO-1* (4.84-fold), *Vinculin* (2.66-fold), *ACE2* (2.41-fold), and *CD31* (1.17-fold) gene expression levels were also clearly decreased due to the disruptive effect of PM2.5 exposure. Supporting WST-1 and LDH assay results, significantly increasing apoptotic *Caspase* (3.10-fold) gene expression level and decreasing cell proliferation markers, *PCNA* (2.69-fold) and

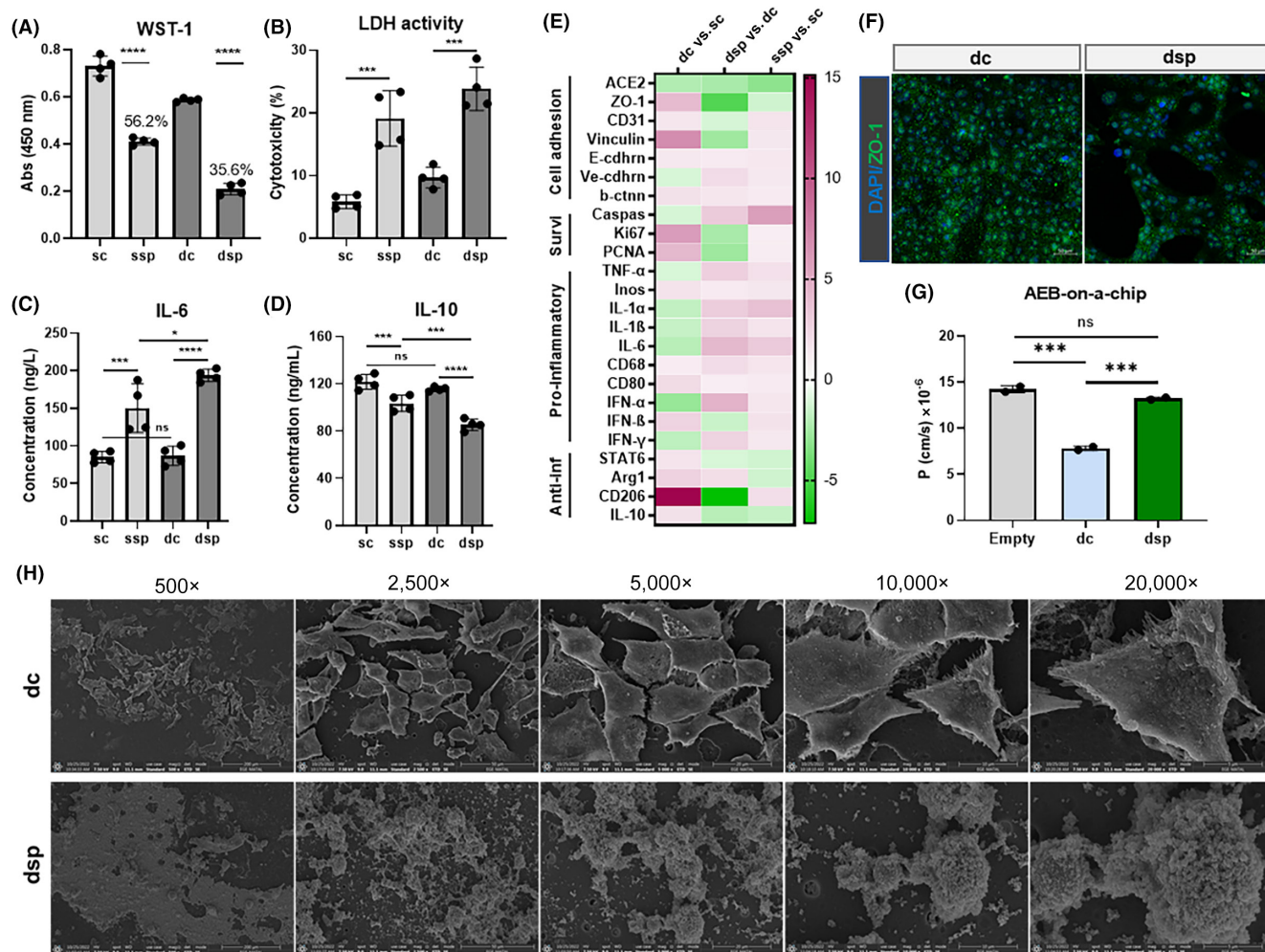


FIGURE 3 PM_{2.5} exposure under dynamic conditions in the on-chip platform disrupts human AEB integrity. The result of (A) WST-1, (B) LDH, (C) IL-6 ELISA, (D) IL-10 ELISA, (ns>.05, **p*<.05, ****p*<.001, *****p*<.0001, *n*=4 for independent replicates=2) (E) the heatmap graph of fold regulation data from qRT-PCR analysis, (F) IF staining of cell markers ZO-1 (scale bars=50μm for 25×, independent replicates=2), (G) FITC permeability assay (ns>.05, ****p*<.001, *n*=2 for independent replicates=2), and (H) SEM analysis of Calu-3 cells on the AEB-on-a-chip platform after 72h of PM_{2.5} exposure (dc: dynamic control, dsp: dynamic silica particles, sc: static control, ssp: static silica particles conditions).

Ki-67 (2.41-fold) levels were shown to impair cell viability effect of PM_{2.5} on dynamic AEB-on-a-chip platform, unlike the comparison of dynamic control group with the static control group. And importantly, a general increase in the expression level of major proinflammatory genes such as *IFN-α* (4.53-fold), *IL-6* (4.2-fold), *IL-1α* (3-fold), *TNF-α* (2.8-fold), *IL-1b* (2.7-fold), *IFN-γ* (2.6-fold), *CD68* (2.1-fold), *Inos* (1.2-fold), and *CD80* (1.1-fold), as well as a clearly decrease in the anti-inflammatory genes such as *CD206* (7.11-fold), *IL-10* (2-fold), and *STAT6* (1.09-fold), were confirmed the presence of subacute proinflammation on Calu-3 cells in dynamic platform, as a result of PM_{2.5} exposure.

3.4 | PM_{2.5} exposed dynamic human airway epithelial barrier-on-a-chip platform exerts barrier disruption

The lack of continuity and decreasing of ZO-1 protein expression of Calu-3 cells, which is localized in the cell membrane and

cell-cell connections, in the dynamic platform, showed that intercellular connections and barrier integrity were impaired as a result of PM_{2.5} exposure (Figure 3F). As a gold standard analysis of barrier integrity, FITC permeability assay was also performed to quantitatively evaluate the effect of PM_{2.5} exposure at elicited dose (800μg/mL) in AEB-on-a-chip platform. A differential effect on Calu-3 epithelial cell barrier permeability was found, where PM_{2.5} exposure to the on-chip platform caused significant increases (*p*<.001) in barrier permeability due to barrier disruption with measured FITC permeability value of 13.2×10^{-6} cm/s, compared to untreated control (7.8×10^{-6} cm/s) (Figure 3G). When SEM images were evaluated, it was seen that PM_{2.5} exposure caused visible adverse changes in the morphology of Calu-3 cells, as apoptotic-like morphology, in dynamic AEB-on-a-chip platform, supporting the hypothesis of disruption in barrier integrity (Figure 3H). All these results showed that dynamic conditions ensured barrier integrity by supporting cell viability and cell adhesion, as well as PM_{2.5} exposure disrupted this barrier integrity and caused a subacute proinflammatory response.

3.5 | PM2.5 exposure causes damage to the healthy human bronchial bronchoscopy biopsy material, resulting in a subacute proinflammatory response

Tissue damage of an ex vivo lung biopsy slices were investigated after PM 2.5 exposure. In this context, the healthy human bronchoscopy bronchial biopsy materials were prepared to use in sterile conditions (Figure 4A) and were cut into ex vivo slices of appropriate size for different applications and analyses (Figure 4B). As a result of PM2.5 exposures for 72h on the slices under dynamic conditions, it was observed that the dispersion occurred and the particles diffused into the slices (Figure 4C), then exerted a cytotoxic effect on the ex vivo tissue with approximately 3.5-fold higher LDH release compared to the control group (Figure 4D). In addition, PM2.5 caused a subacute inflammation, as a significant

increase in the proinflammatory cytokine *IL-6* secretion level ($p < .05$) and a quiet decrease in the anti-inflammatory cytokine *IL-10* (Figure 4E,F). Considering the possible epithelial-endothelial cell barrier integrity in the ex vivo bronchial biopsy sections, qualitatively, ZO-1 expression was evaluated by IF analysis. As a result, while a high level of ZO-1 expression was observed in both PM2.5 treated and untreated control groups, a deterioration in barrier integrity and impaired morphological structure was observed in the tissue layer at the edges of the sections exposed to silica group (Figure 4G). Also, the qRT-PCR analysis was performed for further characterization using such specific markers based on cell adhesion, proliferation, anti-inflammatory, and proinflammatory, after PM2.5 exposure to the biopsy slices for 72h (Figure 4H, Figure S4B and Appendix S2b). The cell-cell, cell-surface adhesion markers, *Vinculin*, *ACE2*, β -catenin, and *E-cadherin* were significantly downregulated by 8.22-fold, 3.35-fold, 2.29-fold, and

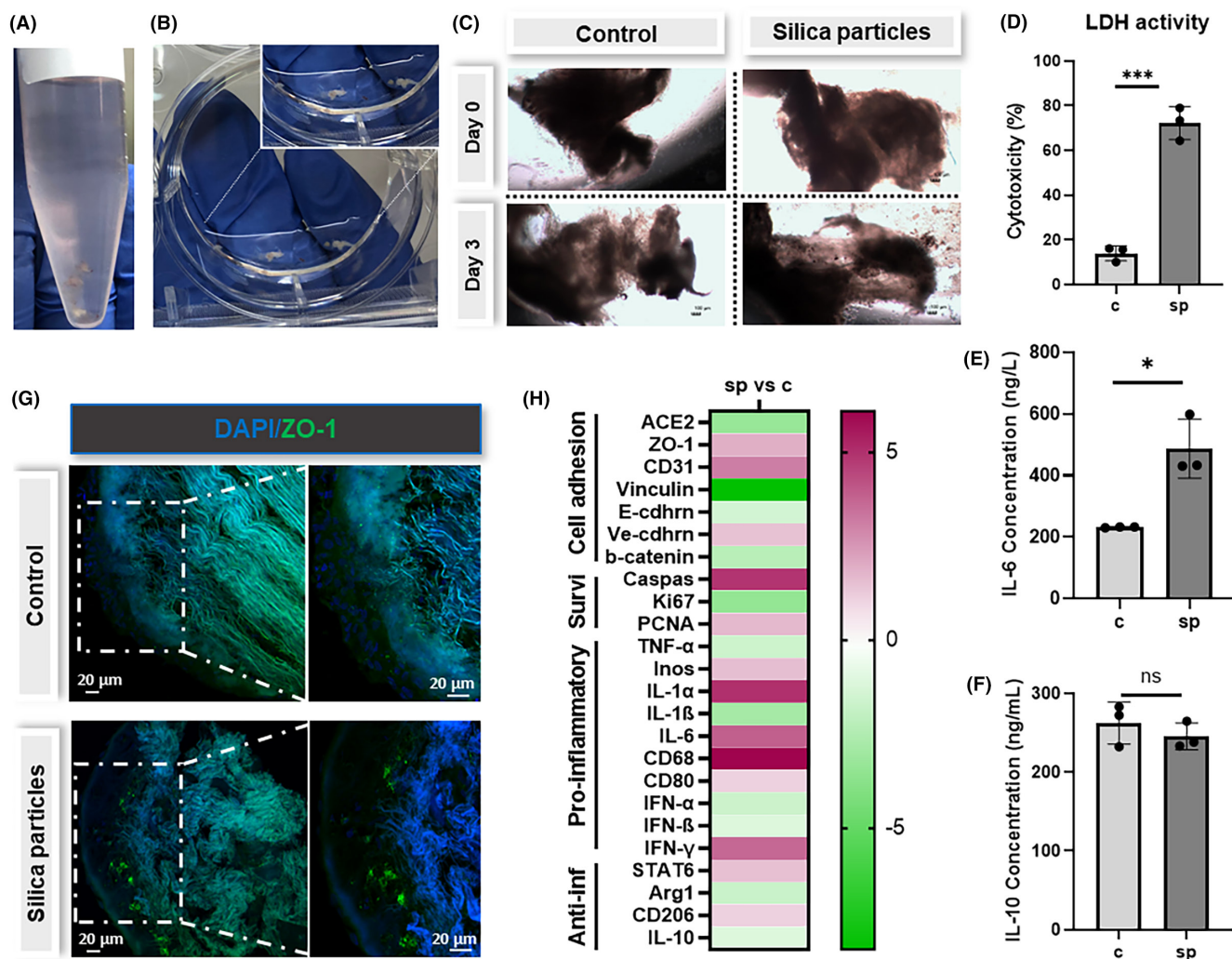


FIGURE 4 Investigation of PM2.5 effect in an ex vivo lung biopsy slice. (A) Healthy human bronchial bronchoscopic biopsy material in sterile saline, (B) dissection of biopsy slices following various washing processes. (C) Bright-field microscopy images (Motic AE31E, bar scale: 100µm), (D) LDH, (E) *IL-6*, (F) *IL-10* ELISA assay results (ns>.05, * $p < .05$, ** $p < .01$, $n = 3$ for independent replicates=2), (G) IF staining (scale bars=20µm for 20 \times and 40 \times magnification images, independent replicates=2) of cell markers ZO-1, and (H) the heatmap graph of fold regulation data from the qRT-PCR analysis, of PM2.5 exposure to biopsy slices under dynamic conditions for 72h (c: control, sp: silica particle).

1.45-fold, respectively, in PM2.5 exposed groups. This event demonstrated that PM2.5 exposure reduced intercellular communication and barrier integrity. Among cell survival markers, *Ki-67* expression was reduced by 3.5-fold, and *Caspase* expression was increased by 4.9-fold after PM2.5 exposure on the biopsy slices, indicating a decrease in cell viability and an increase in cell apoptosis. On the other hand, while the *CD68* (6.1-fold), *IL-1 α* (5-fold), *IL-6* (3.9-fold), *IFN- γ* (3.65-fold), *INOS* (1.6-fold), and *CD80* (1.1-fold) proinflammatory markers were considerably enhanced in ex vivo slices after PM2.5 exposure, compared with the untreated group, the anti-inflammatory markers, *Arg1* and *IL-10* were decreased by 1.77-fold and 1.12-fold, respectively, supporting to ELISA results.

All these results, which were similarly obtained on Calu-3 cells and biopsy tissue, supported the hypothesis that PM2.5 caused a subacute proinflammatory response by causing damage to both the AEB and lung tissue.

4 | DISCUSSION

In our study, two separate but related respirable PM2.5 exposure models, were established and comparatively approached together for the first time, after determining the dose-dependent effect on various lung epithelial cells: (i) a human AEB-on-a-chip model based on simple, easy-to-use, biomimetic, biocompatible, bidirectional and air-liquid interface microfluidic-based platform; and (ii) a human immune cell contained bronchoscopy ex vivo airway model. The inflammatory response to PM2.5 exposure, as well as the disruptive effects on epithelial barrier integrity, were comparatively evaluated in these two models. This study is one of the few examples that highlight the importance of utilizing both in vitro on-chip platforms and ex vivo slices to study the exposure effects of PM2.5 on AEB. The results clearly demonstrate that human airway epithelial barrier of lungs respond dramatically to a PM2.5 dose of 800 $\mu\text{g}/\text{mL}$ in both models, a dose that we can easily be exposed to in real life during extreme weather conditions and natural atmospheric dust transport events.

Changes in external exposomes affecting the epithelial barrier, such as air pollution, exposure to environmental substances, loss of biodiversity play important roles in the formation of allergic diseases.³³ The epithelial barrier theory, which suggests that an increase in agents that damage the epithelial barrier due to environmental conditions causes allergic reactions, requires more experimental models to examine the immune response due to impaired epithelial barrier function as a result of exposure to these agents.^{34,35} Therefore, reliable preclinical models that are used to recapitulate the effects of increasing environmental pollutants such as organic and inorganic dust, microplastics, nanoparticles, bioaerosols, and toxic chemicals from floods and dust storms, which increase due to unplanned urbanization and climate change and affect our lungs directly through the air we breathe, are becoming more and more important on human health in recent years.^{27,36,37} The epithelial barrier defect has just been

categorized as type 5 in the newly expanded classification of Gell and Coombs introduced by the European Academy of Allergy and Clinical Immunology. Type 5 and its hypersensitivity reaction are directly relevant to environmental pollutants and chemicals that disrupt epithelial barriers and have been recently demonstrated in several models and human tissues.^{26,38} Investigating effector mechanisms of environmental factors in advanced feasible models like here, may enable the development of new strategies for prevention and treatment of non/low-type 2 asthma and COPD-like chronic airway diseases associated with environmental dust exposure.

Bioengineered biomimetic microsystem-based lung-on-chip platforms that are created using established cell lines, primary cells derived from human donors, and patient-derived tissue/stem cell-based organoids, allow precise control of exposure conditions, catalyze crucial advances in novel models of lung pathologies and provide a biologically relevant AEB model than traditional in vitro lung models.^{15,21,25,36,39,40} Despite all the state-of-the-art technology, they are still far from providing a totally real lung physiology, have technical and engineering difficulties and need more Food and Drug Administration-approved advances to be recognized by pharmaceutical, regulatory, and academic researchers to abandon their current methods in use. Nevertheless, they have been successfully used as multi-channelled and biosensor integrated microfluidic systems to measure epithelial barrier integrity over the past few years. In this context, Xu et al. presented a 3D human lung-on-a-chip model that recapitulated the structural features of the alveolar-blood barrier through co-culturing of human endothelial cells, epithelial cells, and extracellular matrix, to evaluate PM2.5 exposure. They stated that the monthly average concentration of PM2.5 in an urban area, especially in winter and early spring, can hover around 100–300 $\mu\text{g}/\text{m}^3$. They also argued that since approximately 0.69–0.86 mg of PM2.5 can pass through the adult respiratory tract each day, PM2.5 concentrations of 0–800 $\mu\text{g}/\text{mL}$, commonly used in in vitro toxicity tests in culture media, can be used to recapitulate PM2.5 exposure. The results indicated various malfunctions of the alveolar-capillary barrier, including significantly increased cell cytotoxicity with *AnnexinV*⁺ apoptotic cells, disrupted adherens junction, increased reactive oxygen species generation, inflammatory marker expressions, elevated permeability, and monocyte attachments after an acute high dose of 400 $\mu\text{g}/\text{mL}$ PM2.5 exposure.⁴¹ The level of exposure described significantly surpasses the acceptable limits set by the WHO. However, in the field of exposure science, pivotal factors in disease progression include the duration of exposure and the immune response mechanisms of the affected organism. Responses can also vary depending on the specific type of PM2.5 encountered. As demonstrated in this study, the resilience of the human AEB is notably compromised following exposure to elevated levels of PM2.5 over several days indeed. Special lab-on-chip systems offer a promising approach for investigating the individual effects of prolonged exposure to such concentrations. For instance recently, Park and Young described a novel E-FLOAT platform consisting of airway

epithelium cultured on a floating hydrogel layer secured by micro-fabricated anchors within a microfluidic chip, which is very compatible with PM exposure studies. Their model is an extractable floating liquid gel-based dynamic perfused lung-on-a-chip platform with 0.026 dyn/cm^2 shear stress for airway tissue modeling with submerged Calu-3 cells to clearly evaluate PM_{2.5} deposition on cells and investigates improved physiologic mimicry in airway epithelium composition, tight junction expression, mucus production, and cilia formation of cells.⁴² However, they could not evaluate the cell destructive, increased permeability, and inflammatory effects of PM_{2.5} exposure on their on-chip model, unlike in our on-chip model that has $2 \times 10^{-4} \text{ dyn/cm}^2$ shear stress.

On the other hand, human precision-cut lung slices (PCLS), which are one of the best ex vivo organotypic tissue models, mimic living lung environment, bridge the gap between in vivo and in vitro models, and provide the opportunity to investigate the respiratory tract containing all lung cell types.^{22,43–46} In this context, bronchial biopsy-derived small ex vivo slices have been used for the prevention and treatment of such clinical lung diseases, especially acute lung injury, asthma, and COPD studies, for many years to investigate the respiratory tract that contains such epithelium, immune-related, basement membrane, and smooth muscle cells. Henjakovic et al.⁴⁷ evaluated the changes in cytokine production and the expression of cell-surface markers of PCLS after immunoactive substances exposure such as lipopolysaccharides. Similar to our study, LDH activation and typical proinflammatory stimuli have been shown to notably increase by elevated levels of *IL-1 α* and *TNF- α* on PCLS, and they suggested that PCLS may stand out as a suitable ex vivo technique to predict the immunomodulatory potency of inhaled substances. Similarly, Kim et al.⁴⁸ investigated the toxic and inflammatory effects of exposure to some nanoparticles including silica, on both ex vivo mouse PCLS, mice and in vitro macrophages. Silica nanoparticles significantly led to LDH active toxicity and mainly *IL-6*-derived proinflammatory responses on PCLS, in a size- and chemical composition-dependent manner.

The hemodynamic forces such as shear stress and fluid distribution regulating mechanosensitive signals are known to regulate important structural organogenesis. Thus, in silico simulation of shear stress is quite important for on-chip platforms with the use of biology and engineering principles that can emulate the spatio-temporal dynamics and cell–cell, cell–environment interactions.⁴⁹ Besides comparison of our newly designed and easy-to-use on-chip platform with a human airway ex vivo model in barrier integrity, toxicity and inflammatory manner, modeling of dynamic flow conditions using COMSOL Multiphysics allowed reliable verification of the study results. Then, we evaluated the disruptive effect of respirable PM_{2.5} exposure on epithelial barrier integrity in molecular, biological, and functional manner in our on-chip and ex vivo slice models, as in equivalent cell culture systems and animal models. Notably, we elicited subacute proinflammatory effect of dust exposure via increasing expression levels of most important proinflammatory-related genes of *IFNs*, *IL-6*, *IL-1s*, *TNF- α* , *CD68*,

CD80, and *Inos* on airway epithelial cells in dynamic AEB-on-a-chip model, as well as *CD68*, *IL-1 α* , *IL-6*, *IFN- γ* , *Inos*, and *CD80* genes on tissue slices in ex vivo model. Exposure to dust particles significantly initiates inflammation of the airways not only for asthmatic patients but also for healthy subjects.⁵⁰ As in many other studies, Williams et al.²⁷ stated that the major proinflammatory cytokine, *IL-6* release, was highly increased and had a proinflammatory effect in BEAS-2B and A549 lung epithelial cells after exposure to silica particles, while Xu et al.⁴¹ measured increasing levels of both *IL-6* and *TNF- α* derived proinflammatory response in their on-chip model after PM_{2.5} exposure, similar to our on-chip and ex vivo models.

Common anti-inflammatory immune cell markers such as *CD206*, *Arg1*, *IL-10*, and *STAT6* that play roles in the regulation of the immune response and tissue repair, are usually decreased in active proinflammatory response,^{28,51} like in our study. Notably, *STAT6* expression significantly decreased in our AEB-on-a-chip model but quite increased in our ex vivo slice model as unexpected, unlike other markers. In the literature, it is mentioned that *STAT6* also mediates the biological effects of TH2 cytokines, plays an important role in the pathogenesis of asthma and is expressed in many different immune cell types involved in allergic lung inflammation. There is abundant evidence that *STAT6* promotes allergic lung disease, and Ihrie et al.⁵² showed that *STAT6* also contributes to exacerbation of house dust mite allergen-induced allergic airway disease by multi-walled carbon nanotubes in mice. In another study, Natarajan et al.³⁷ mentioned that the increased *STATs* activity mediates cellular signaling mechanisms from such cytokines and growth factors and strengthens the inflammatory side, while the different *STATs* activation can be monitored in different cell lines, models, type of dust, and the onset and duration of *STATs* activation may be due to different control of the protein tyrosine phosphatase responsible for redox regulation. They concluded that the increasing *STAT3* activity enhanced both *IL-6*, *TNF- α* , and *IL-1* levels after organic dust exposure in their mice model. Therefore, in contrast to our in vitro model, the increase in *STAT6* level after inorganic dust exposure for 72 h in the ex vivo model containing immune cells was considered reasonable.

The study results have established a dose of $800 \mu\text{g/mL}$, which significantly compromises the resilience of the epithelial barrier. While extrapolating from in vitro concentrations to human exposures is challenging, this dose exceeds the normal daily permissible exposure limits set by the WHO but corresponds to a high level of exposure observed in atmospheric monitoring studies during extreme weather conditions. Determining this critical level of exposure to PM_{2.5} in a biomimetic AEB-on-a-chip model is one of the original contributions of the study. Organ-on-chip systems mimic organ-specific functions and are potential alternative pre-clinical models compared to conventional 2D in vitro and in vivo animal models for environmental exposure studies indeed. They provide required spatial, mechanical, and chemical cues for cell dynamics with advantages of high-throughput drug screening. On the other hand, microfluidic devices for organ-on-chip studies can

be challenging to researchers in basic sciences with limited technical background. Because dynamic factors and physical forces in the channels of the on-chip platform or the whole system that can be fabricated and assembled with engineering approaches may exert difficulties during the entire experiment. Furthermore, labor-intensive, complexly designed on-chip platforms with high initial manufacturing costs may bring extra difficulties to work with these on-chip models. Therefore, automated, easy-to-set, basically designed and sensor-integrated organ-on-chip platforms for real-time measurement of pH, oxygen, temperature, and various extracellular metabolites can be streamlined without relying on manual operation to enhance the reproducibility and accurate sensing of organ models. These limitations can be overcome with the coordinated studies resulting from translational interdisciplinary convergence of engineers and scientists from various disciplines.^{39,51,53}

5 | CONCLUSION

Airborne PM with inorganic components stands out as a significant future respiratory hazard for human AEB under climate change conditions. In our study, PM_{2.5} exposures simultaneously activated *IFNs*, *IL-6*, *IL-1s*, *TNF-α*, *CD68*, *CD80*, *Inos* positive and *CD206*, *IL-10*, *STAT6* negative subacute proinflammation, caused *ZO-1*, *Vinculin*, *ACE2*, and *CD31* negative barrier disruption with increased FITC permeability and *Caspase-3/Ki-67/PCNA*-epithelial cell toxicity in our newly designed easy-to-use AEB-on-a-chip platform, while it enhanced both *CD68*, *IL-1α*, *IL-6*, *IFN-γ*, *Inos*, *CD80* positive and *IL-10*, *Arg1* negative subacute proinflammation with *Caspase-3/Ki67*-apoptotic identity and *Vinculin*, *ACE2*, *β-catenin*, *E-cadherin* negative impaired tissue structure in ex vivo biopsy slices. All our results suggested that PM_{2.5} exposures caused different cell type activation that modulate different molecular pathways related to subacute proinflammation and cell-tissue toxicity in our on-chip and ex vivo models. A better understanding of the mechanisms by which types of inhalable agents predominantly disrupt the AEB, and for whom and for how long such disruptions occur in such contexts, may enable the development of new strategies for the prevention and treatment of chronic airway diseases such as asthma and COPD associated with dust exposure.

AUTHOR CONTRIBUTIONS

I.S., S.B., O.G., P.S.M., and O.Y.C. conceived the study. I.S., P.S.-M., S.Y., and S.B. performed the general experiments. T.G. performed the lung biopsy. C.B.-A., L.S.T., and M.S.-T. analyzed the PCR data. P.S.-M., S.Y., and I.S. wrote and revised the manuscript, and O.G., T.G., and O.Y.-C. reviewed and edited the manuscript.

ACKNOWLEDGMENTS

We sincerely thank Professor Dr.Tuncay Goksel (T.G.) from the Department of Pulmonary Medicine at Ege University and

Translational Pulmonary Research Center (EgeSAM) for his valuable contributions to obtaining bronchial biopsy samples. S.Y. and P.S.M. acknowledge the TUBITAK 2210-C and TUBITAK 2211-A National Graduate Scholarship Programs, respectively.

FUNDING INFORMATION

The funding was provided by the Presidency of the Republic of Turkey Strategy and Budget Department (2019K12-149080) and the Scientific and Technological Research Council of Turkey (TUBITAK) under grant number 1139B412102522.

CONFLICT OF INTEREST STATEMENT

The authors declare that the research was conducted in the absence of any commercial or financial relationships that could be construed as a potential conflict of interest.

DATA AVAILABILITY STATEMENT

The original contributions presented in the study are included in the main manuscript/supplementary information. Further inquiries can be directed to the corresponding author.

ORCID

Ozlem Goksel  <https://orcid.org/0000-0003-1121-9967>

Sena Yanasik  <https://orcid.org/0000-0002-5685-3737>

REFERENCES

- Pawankar R, Akdis CA. Climate change and the epithelial barrier theory in allergic diseases: a one health approach to a green environment. *Allergy*. 2023;78(11):2829-2834.
- D'Amato G, Akdis CA. Desert dust and respiratory diseases: further insights into the epithelial barrier hypothesis. *Allergy*. 2022;77(12):3490-3492.
- Goshua A, Akdis CA, Nadeau KC. World Health Organization global air quality guideline recommendations: executive summary. *Allergy*. 2022;77(7):1955-1960.
- Boğan M, Kul S, Al B, et al. Effect of desert dust storms and meteorological factors on respiratory diseases. *Allergy*. 2022;77(7):2243-2246.
- Movassagh H, Prunicki M, Kaushik A, et al. Proinflammatory polarization of monocytes by particulate air pollutants is mediated by induction of trained immunity in pediatric asthma. *Allergy*. 2023;78(7):1922-1933.
- Aguilera J, Han X, Cao S, et al. Increases in ambient air pollutants during pregnancy are linked to increases in methylation of *IL4*, *IL10*, and *IFNγ*. *Clin Epigenetics*. 2022;14(1):40.
- Lwin KS, Tobias A, Chua PL, et al. Effects of desert dust and sandstorms on human health: a scoping review. *Geohealth*. 2023;7(3):e2022GH000728.
- World Health Organization. *Air Quality Guidelines—Update 2021*. WHO Regional Office for Europe; 2021.
- Pai SJ, Carter TS, Heald CL, Kroll JH. Updated World Health Organization air quality guidelines highlight the importance of non-anthropogenic PM_{2.5}. *Environ Sci Technol Lett*. 2022;9(6):501-506.
- Katra I, Krasnov H. Exposure assessment of indoor PM levels during extreme dust episodes. *Int J Environ Res Public Health*. 2020;17(5):1625.

11. Nawahda A. The impact of extremely high levels of PM_{2.5} on surface ozone during massive dust storms. *Kuwait J Sci.* 2023;50(4):717-723.
12. Copernicus Atmosphere Monitoring Service. Extreme episode of particulate matter air pollution across Italy's Po Valley. 2024. Accessed April 4, 2024. <https://atmosphere.copernicus.eu/extreme-episode-particulate-matter-air-pollution-across-italys-po-valley>
13. Johnston SL, Goldblatt DL, Evans SE, Tuvim MJ, Dickey BF. Airway epithelial innate immunity. *Front Physiol.* 2021;12:749077.
14. Rathnayake SNH, Ditz B, van Nijnatten J, et al. Smoking induces shifts in cellular composition and transcriptome within the bronchial mucus barrier. *Respirology.* 2023;28(2):132-142.
15. Benam KH, Novak R, Ferrante TC, Choe Y, Ingber DE. Biomimetic smoking robot for in vitro inhalation exposure compatible with microfluidic organ chips. *Nat Protoc.* 2020;15(2):183-206.
16. Cao X, Muskhelishvili L, Latendresse J, Richter P, Heflich RH. Evaluating the toxicity of cigarette whole smoke solutions in an air-liquid-interface human in vitro airway tissue model. *Toxicol Sci.* 2017;156(1):14-24.
17. Landwehr KR, Hillas J, Mead-Hunter R, et al. Toxicity of different biodiesel exhausts in primary human airway epithelial cells grown at air-liquid interface. *Sci Total Environ.* 2022;832:155016.
18. Frieke Kuper C, Gröllers-Mulderij M, Maarschalkerweerd T, et al. Toxicity assessment of aggregated/agglomerated cerium oxide nanoparticles in an in vitro 3D airway model: the influence of mucociliary clearance. *Toxicol In Vitro.* 2015;29(2):389-397.
19. Rothen-Rutishauser B, Blank F, Mühlfeld C, Gehr P. In vitro models of the human epithelial airway barrier to study the toxic potential of particulate matter. *Expert Opin Drug Metab Toxicol.* 2008;4(8):1075-1089.
20. Shakya S, Pyles KD, Albert CJ, Patel RP, McCommis KS, Ford DA. Myeloperoxidase-derived hypochlorous acid targets human airway epithelial plasmalogens liberating protein modifying electrophilic 2-chlorofatty aldehydes. *Redox Biol.* 2023;59:102557.
21. Saygili E, Yildiz-Ozturk E, Green MJ, Ghaemmaghami AM, Yesil-Celiktas O. Human lung-on-chips: advanced systems for respiratory virus models and assessment of immune response. *Biomicrofluidics.* 2021;15(2):021501.
22. Saglam-Metiner P, Yildiz-Ozturk E, Tetik-Vardarli A, et al. Organotypic lung tissue culture as a preclinical model to study host-influenza A viral infection: a case for repurposing of nafamostat mesylate. *Tissue Cell.* 2024;87:102319.
23. Saygili E, Devamoglu U, Bayir E, Yesil-Celiktas O. An optical pH-sensor integrated microfluidic platform multilayered with bacterial cellulose and gelatin methacrylate to mimic drug-induced lung injury. *J Ind Eng Chem.* 2023;121:190-199.
24. Jung O, Tung YT, Sim E, et al. Development of human-derived, three-dimensional respiratory epithelial tissue constructs with perfusable microvasculature on a high-throughput microfluidics screening platform. *Biofabrication.* 2022;14(2):025012.
25. Zhou Y, Duan Q, Yang D. In vitro human cell-based models to study airway remodeling in asthma. *Biomed Pharmacother.* 2023;159:114218.
26. Saito K, Orimo K, Kubo T, et al. Laundry detergents and surfactants-induced eosinophilic airway inflammation by increasing IL-33 expression and activating ILC2s. *Allergy.* 2023;78(7):1878-1892.
27. Williams LJ, Zosky GR. The inflammatory effect of iron oxide and silica particles on lung epithelial cells. *Lung.* 2019;197(2):199-207.
28. Saygili E, Saglam-Metiner P, Cakmak B, et al. Bilayered laponite/alginate-poly(acrylamide) composite hydrogel for osteochondral injuries enhances macrophage polarization: an in vivo study. *Biomater Adv.* 2022;134:112721.
29. Ilhan-Ayisigi E, Saglam-Metiner P, Sancı E, et al. Receptor mediated targeting of EGF-conjugated alginate-PAMAM nanoparticles to lung adenocarcinoma: 2D/3D in vitro and in vivo evaluation. *Int J Biol Macromol.* 2024;261:129758.
30. Agarwal S, Plesco NP, Johns LP, Riccelli AE. Differential expression of IL-1 β , TNF- α , IL-6, and IL-8 in human monocytes in response to lipopolysaccharides from different microbes. *J Dent Res.* 1995;74(4):1057-1065.
31. Segura M, Vadeboncoeur N, Gottschalk M. CD14-dependent and -independent cytokine and chemokine production by human THP-1 monocytes stimulated by *Streptococcus suis* capsular type 2. *Clin Exp Immunol.* 2002;127(2):243-254.
32. Ishijima T, Nakajima K. Inflammatory cytokines TNF α , IL-1 β , and IL-6 are induced in endotoxin-stimulated microglia through different signaling cascades. *Sci Prog.* 2021;104(4):003685042110549.
33. Celebi Sozener Z, Ozdel Ozturk B, Cerci P, et al. Epithelial barrier hypothesis: effect of the external exposome on the microbiome and epithelial barriers in allergic disease. *Allergy.* 2022;77(5):1418-1449.
34. Akdis CA. Does the epithelial barrier hypothesis explain the increase in allergy, autoimmunity and other chronic conditions? *Nat Rev Immunol.* 2021;21(11):739-751.
35. Ogulur I, Yazici D, Pat Y, et al. Mechanisms of gut epithelial barrier impairment caused by food emulsifiers polysorbate 20 and polysorbate 80. *Allergy.* 2023;78(9):2441-2455.
36. Wang H, Yin F, Li Z, Su W, Li D. Advances of microfluidic lung chips for assessing atmospheric pollutants exposure. *Environ Int.* 2023;172:107801.
37. Natarajan K, Meganathan V, Mitchell C, Boggaram V. Organic dust induces inflammatory gene expression in lung epithelial cells via ROS-dependent STAT-3 activation. *Am J Physiol Lung Cell Mol Physiol.* 2019;317:127-140.
38. Jutel M, Agache I, Zemelka-Wiacek M, et al. Nomenclature of allergic diseases and hypersensitivity reactions: adapted to modern needs: an EAACI position paper. *Allergy.* 2023;78(11):2851-2874.
39. Ingber DE. Human organs-on-chips for disease modelling, drug development and personalized medicine. *Nat Rev Genet.* 2022;23(8):467-491.
40. Yildiz-Ozturk E, Saglam-Metiner P, Yesil-Celiktas O. Lung carcinoma spheroids embedded in a microfluidic platform. *Cytotechnology.* 2021;73(3):457-471.
41. Xu C, Zhang M, Chen W, Jiang L, Chen C, Qin J. Assessment of air pollutant PM_{2.5} pulmonary exposure using a 3D Lung-on-Chip model. *ACS Biomater Sci Eng.* 2020;6(5):3081-3090.
42. Park S, Young EWK. E-FLOAT: extractable floating liquid gel-based organ-on-a-Chip for airway tissue modeling under airflow. *Adv Mater Technol.* 2021;6(12):2100828.
43. Murugan AT, Calhoun WJ. Invasive tests: Bronchoalveolar lavage and biopsy: the scope of the scope. *Clinical Asthma.* Elsevier; 2008:107-116.
44. Lauenstein L, Switalla S, Prenzler F, et al. Assessment of immunotoxicity induced by chemicals in human precision-cut lung slices (PCLS). *Toxicol In Vitro.* 2014;28(4):588-599.
45. Liu Y, Wu P, Wang Y, et al. Application of precision-cut lung slices as an in vitro model for research of inflammatory respiratory diseases. *Bioengineering.* 2022;9(12):767.
46. Sun Y, Jing P, Gan H, et al. Evaluation of an ex vivo fibrogenesis model using human lung slices prepared from small tissues. *Eur J Med Res.* 2023;28(1):143.
47. Henjakovic M, Sewald K, Switalla S, et al. Ex vivo testing of immune responses in precision-cut lung slices. *Toxicol Appl Pharmacol.* 2008;231(1):68-76.
48. Kim YH, Boykin E, Stevens T, Lavrich K, Gilmour MI. Comparative lung toxicity of engineered nanomaterials utilizing in vitro, ex vivo and in vivo approaches. *J Nanobiotechnol.* 2014;12(1):47.
49. Saglam-Metiner P, Devamoglu U, Filiz Y, et al. Spatio-temporal dynamics enhance cellular diversity, neuronal function and further maturation of human cerebral organoids. *Commun Biol.* 2023;6(1):173.

50. Simeone-Penney MC, Severgnini M, Tu P, et al. Airway epithelial STAT3 is required for allergic inflammation in a murine model of asthma. *J Immunol.* 2007;178(10):6191-6199.
51. Saglam-Metiner P, Duran E, Sabour-Takanlou L, Biray-Avci C, Yesil-Celiktas O. Differentiation of neurons, astrocytes, oligodendrocytes and microglia from human induced pluripotent stem cells to form neural tissue-on-chip: a neuroinflammation model to evaluate the therapeutic potential of extracellular vesicles derived from mesenchymal stem cells. *Stem Cell Rev Rep.* 2024;20(1):413-436.
52. Ihrie MD, Duke KS, Shipkowski KA, et al. STAT6-dependent exacerbation of house dust mite-induced allergic airway disease in mice by multi-walled carbon nanotubes. *NanoImpact.* 2021;22:100309.
53. Saglam-Metiner P, Yildirim E, Dincer C, Basak O, Yesil-Celiktas O. Humanized brain organoids-on-chip integrated with sensors for screening neuronal activity and neurotoxicity. *Microchim Acta.* 2024;191(1):71.

SUPPORTING INFORMATION

Additional supporting information can be found online in the Supporting Information section at the end of this article.

How to cite this article: Goksel O, Sipahi MI, Yanasik S, et al.

Comprehensive analysis of resilience of human airway epithelial barrier against short-term PM2.5 inorganic dust exposure using in vitro microfluidic chip and ex vivo human airway models. *Allergy.* 2024;00:1-13. doi:[10.1111/all.16179](https://doi.org/10.1111/all.16179)